NANO EXPRESS

The Fabrication of Nano-Particles in Aqueous Solution From Oxyfluoride Glass Ceramics by Thermal Induction and Corrosion Treatment

Hua Yu · Nan Hu · Ya-Nan Wang ·
Zi-Lan Wang · Zong-Song Gan · Li-Juan Zhao

Abstract An innovative route is reported to fabricate nano-particles in aqueous solution from oxyfluoride glass by the thermal induction and corrosion treatment in this letter. The investigations of X-ray diffraction and transmission electron microscope based on nano-particles in glass ceramics (GCs) and aqueous solution indicate that the nano-particles formed in glass matrix during the thermal induction process are released to aqueous solution and their structure, shape and luminescent properties in glass host can be kept. Owing to the designable composition of the nano-particles during glass preparation process, the method is a novel way to obtain nano-particles in aqueous solution from GCs.

Keywords Nano-particles · Glass ceramics ·
Thermal induction and corrosion treatment

Introduction

Since Wang and Ohwaki [1] reported that transparent oxyfluoride glass ceramics (GCs) showed more efficient

H. Yu (✉) · N. Hu · Y.-N. Wang · Z.-L. Wang · Z.-S. Gan ·
L.-J. Zhao (✉)
Photonics Center, College of Physical Science,
Nankai University, Tianjin 300071, China
e-mail: yuhua@nankai.edu.cn

L.-J. Zhao
e-mail: zhaolj@nankai.edu.cn

H. Yu · L.-J. Zhao
Tianjin Key Lab of Photonics Material and Technology for
Information Science and The Key Lab of Weak Light Nonlinear
Photonics, Ministry of Education, Nankai University,
Tianjin 300457, China

upconversion (UC) from infrared to visible than fluoride glass in 1993, many researchers have paid attention to oxyfluoride GCs. [2–5] The advantages of these materials are that the rare earth (RE) ions can be incorporated selectively in the fluoride crystal phase with lower phonon energy after thermal induction and the materials remain transparent due to the nano-scale size of precipitated crystals much smaller than the wavelength of visible light.

Unlike multiphoton absorption in organic dyes or semiconductor quantum dots (QDs), photon UC involves real intermediate quantum states to generate efficient visible light by near infrared (NIR) excitation. High-efficient luminescent intensity, adjustable size, narrow size distribution and unique optical properties are helpful to practical applications of UC materials, especially RE-ion-doped inorganic nano-particles after heat-treatment, in the fields of flat-panel display, light-emitting diodes, temperature sensors, biolabels, DNA detection, photodynamic therapy, etc [6–10]. Moreover, different nano-particles composition could be designed in glass matrix [11–14]. Unfortunately, ever since the first report on oxyfluoride GCs, there have been much research on the properties of nano-particles in GCs but no publication has been reported about how to obtain free nano-particles in aqueous solution from the GC-host and how to apply it to the fields mentioned above, especially in biological field. Therefore, it is of great significance to develop convenient routes to fabricate inorganic nano-particles doped RE-ion in aqueous solution from GCs in order to meet their practical application requirements.

Silicate oxyfluoride glass is selected here and $(Pb,Cd)F_2:Er^{3+},Yb^{3+}$ nano-particles were formed in glass matrix after thermal induction. Acid corrosion treatment was employed to remove the glass matrix in order to obtain free $(Pb,Cd)F_2:Er^{3+},Yb^{3+}$ nano-particles in aqueous

solution. The UC emissions of $(Pb,Cd)F_2:Er^{3+},Yb^{3+}$ nano-particles in aqueous solution have been well characterized by pumping the intermediate $^4I_{11/2}$ state of the Er^{3+} ion via a facile 980 nm NIR diode laser. The 980 nm excitation wavelength is fairly transparent for most large biomolecules and does no damage to them. The UC emissions of $(Pb,Cd)F_2:Er^{3+},Yb^{3+}$ nano-particles in aqueous solution are convenient to observe. Additionally, different nano-particles composition and different RE-ion-dope can be employed for cellular and intracellular target.

Experimental Details

Oxyfluoride glasses with composition of $45.5SiO_2$–$40PbF_2$–$10CdF_2$–$0.5Er_2O_3$–$4Yb_2O_3$ were prepared. About 20 g of starting material were fully mixed and melted in a covered platinum crucible in air atmosphere at 1,000 °C for 2 h, and then cast into a steel plate. [1–5] To obtain nano-particles in glass ceramic, the glass samples were subsequently heat-treated at 470 °C for 8 h at the nucleation temperature measured by differential thermal analysers (DTA). Using DTA equipment (TA-Inst 2100), samples were held in a Pt crucible and analysed against a calcined Al_2O_3 reference at a heating rate of 20 °C min^{-1}. The nano-particles in aqueous solution were fabricated with the following method. Firstly, the GCs (about 500 mg) were immersed into 5.65 mol/L hydrofluoric acid for 20 h to get rid off silicate glass host. After corrosion treatment, the nano-particles were deposited by solid–liquid separation. Then pH value was adjusted to neutrality by repeated adding distilled water. Finally, the nano-particles in aqueous solution were dispersed using sodium lauryl benzenesulphate. A small quantity of the dried nano-particles powder was used for X-ray diffraction (XRD) measurements, while a dilute solution of the dispersed powder in distilled water was used for fluorescent and shape studies. XRD analysis were performed to identify the crystallization phase with a power diffractometer (D/Max-2500), using CuKα as the radiation. The 2θ scan range was 5–85° with a step size of 0.02°. Fluorescent spectra were measured with SPEX Fluorolog-2 Spectrofluorimeter (with error ± 0.2 nm), in which 980 nm semiconductor laser is the excitation source and a photo-multiplier tube is the detector. In order to compare the intensity of the luminescence of all the samples as accurately as possible, the position and power of the pumping beam and the width of the slit to collect the luminescence signal were fixed under the same conditions. All the measurements were carried out at room temperature. The preparation and measurement process for all samples are the same conditions.

Results and Discussion

Figure 1a shows the XRD pattern of the investigated GCs. After thermal induction, the XRD pattern of GCs presented intense diffraction peaks, which can be easily assigned to the β-$(Pb,Cd)F_2:Er^{3+},Yb^{3+}$ phase [15]. The lattice constant of β-PbF_2 crystal with the fluorite structure is $a = 0.575$ nm. The slightly smaller lattice constant of the present nano-particles may be interpreted by assuming that the nano-particles are a β-PbF_2 solid solution in which Pb^{2+} ions with ionic radius of 0.129 nm are partially substituted by Cd^{2+} ions whose ionic radius is 0.097 nm and RE-ion with ionic radius about 0.100 nm. [15] This result is further supported by TEM of our glass-ceramics shown in Fig. 1b. The micrograph reveals that nano-particles are uniformly dispersed in a glass matrix. Furthermore, the particle size distribution has been shown in Fig. 1c. The average size of as-prepared nano-particles determined from TEM image is 42.6 nm.

The nano-particles in aqueous solution were obtained by hydrofluoric acid corrosion treatment, adjusting pH value and dispersion of surface active agent. Figure 2 shows the XRD spectrum and TEM image of nano-particles after corrosion treatment process. Phase identification of the nano-particles has been studied by using XRD. The typical XRD patterns show strong diffraction peaks that can be indexed to the β-$(Pb,Cd)F_2:Er^{3+},Yb^{3+}$ phase due to the appreciable shift of XRD peaks position and former research results [15, 16]. No additional or intermediate phase is detected in the sample. The peaks position and half peak breadth of XRD are in concordance with those measured in GCs, which indicates that nano-particles are released from glass matrix to aqueous solution. Moreover, the baseline of XRD is nearly a straight line compared with that of XRD of GCs, which also indicates that silicate glass host is corroded completely. The Fig. 2b is the TEM image of nano-particles in aqueous solution and Fig. 2c reveals the size distribution. The average particle size is obtained as 41.7 nm, which is very close to the former calculation result of nano-particles existing in glass matrix 42.6 nm. And the comparison of Figs. 1 and 2 indicates that the nano-particles formed in glass matrix are released to aqueous solution and their structure, shape and size distribution in glass host are kept well. The potential reason could be the restriction of glass mesh structure during the thermal induction process. The nano-particles exhibit a narrow size distribution and display a good dispersibility in aqueous solution.

Figure 3 reveals the main UC emission of the $^2H_{11/2}/^4S_{3/2}/^4F_{9/2} \rightarrow {}^4I_{15/2}$ transition in GCs and in aqueous solution under 980 nm diode laser excitation. The weak ultraviolet UC radiation of the $^4G_{11/2} \rightarrow {}^4I_{15/2}$ transition were not shown here, since we focus on the ratio of red and

Fig. 1 a XRD patterns of GCs after thermal induction. The asterisks correspond to JCPDS file NO.06-0251 (β-PbF$_2$). b TEM micrographs of nano-particles existing in glass matrix. c .The size distribution of nano-particles in glass matrix
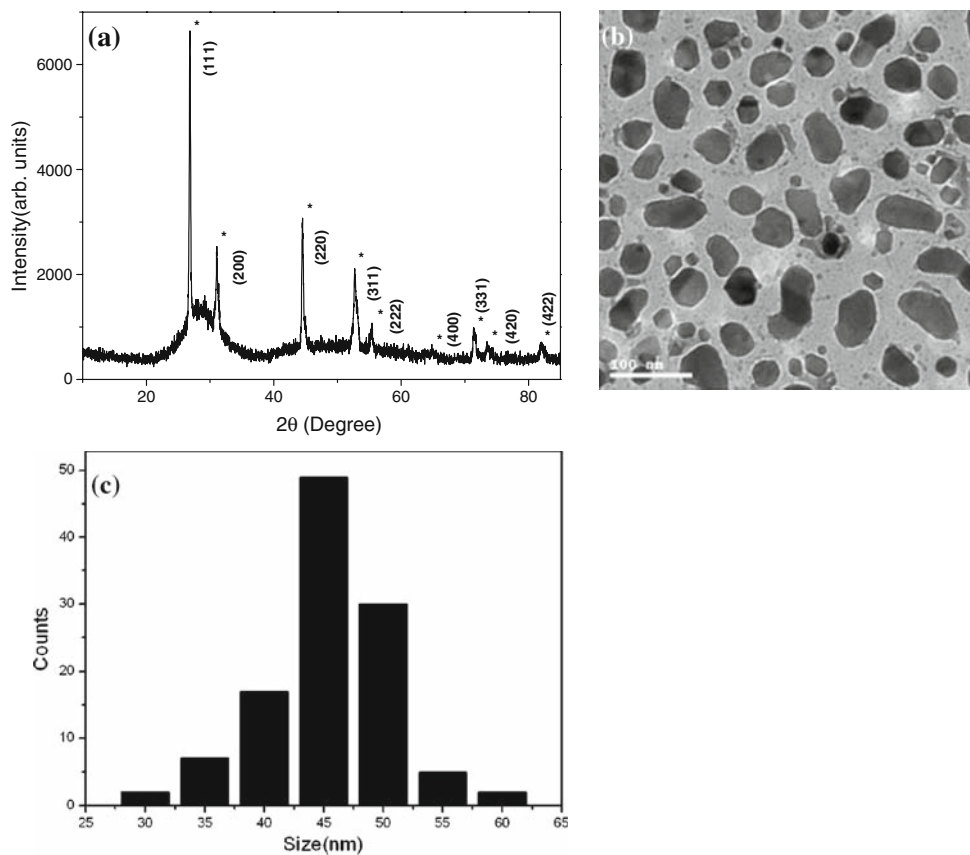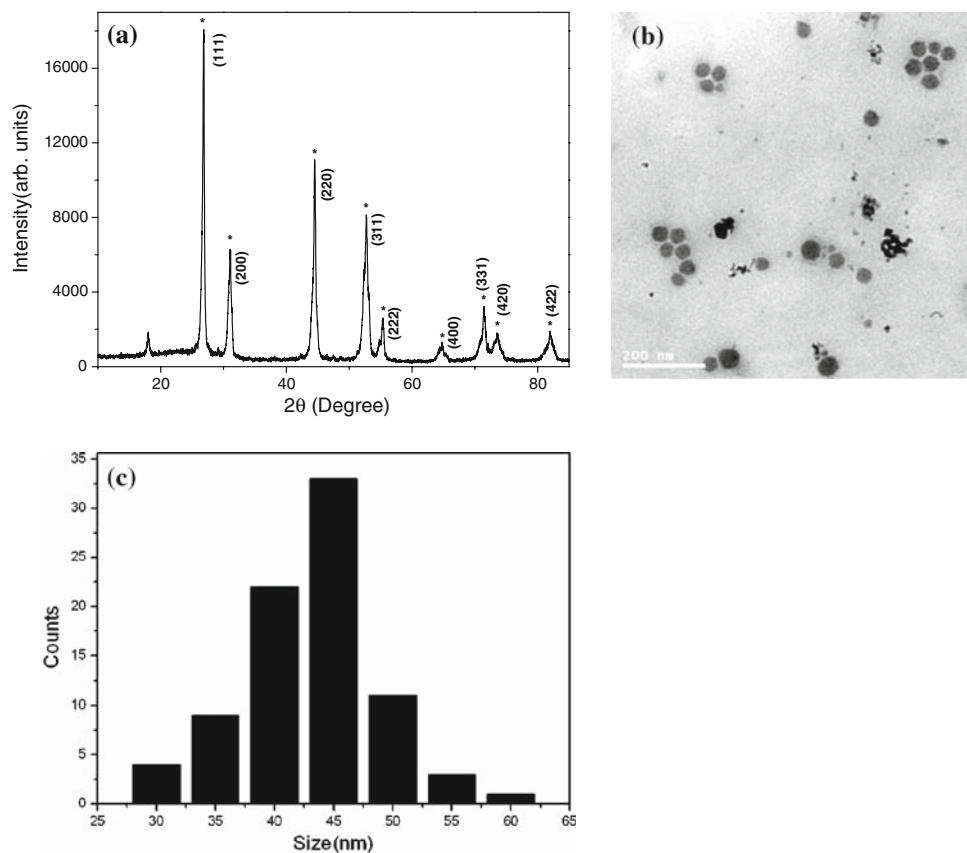

Fig. 2 a XRD patterns of dried nano-particles after corroding treatment. The asterisks correspond to JCPDS file NO.06-0251 (β-PbF$_2$). b TEM micrographs of nano-particles, showing highly dispersive nano-scale quasi-sphere. c The size distribution of nano-particles in aqueous solution
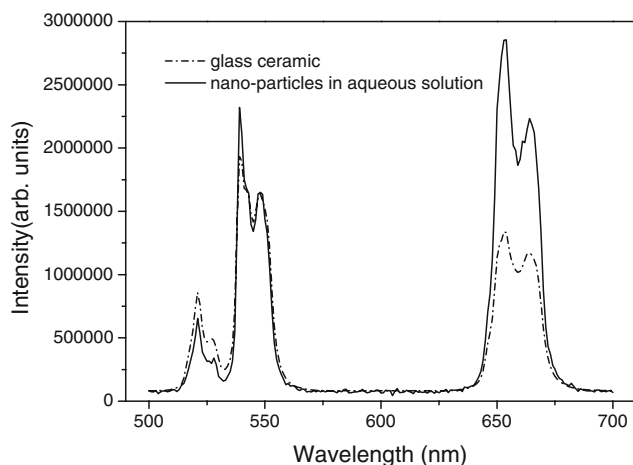
Fig. 3 Measured UC red and green emission in GCs and nano-particles in aqueous solution under diode laser excitation of 980 nm

green fluorescent intensities, which could show the variation of crystal lattice field around the RE-ion. Compared to GCs, the red fluorescent intensity of nano-particles in aqueous solution dramatically increases as shown in Fig. 3. The UC mechanisms of the green and red emissions had been researched by our groups [16, 17]. And the Er^{3+} ion can be promoted to the $^4I_{11/2}$ state through ground state absorption (GSA) of laser photons, and then to the $^2H_{11/2}$ state by use of the excited state absorption (ESA) or energy transfer UC (ETU) processes. The $^4S_{3/2}$ state can also be populated by relaxations from the upper $^2H_{11/2}$ state. The green luminescence is emitted by the transition from $^2H_{11/2}$ and $^4S_{3/2}$ state to $^4I_{15/2}$ ground state. Hence, the green UC luminescence seldom subjects to influence of phonon energy difference of crystal field around the RE ions. The red UC luminescence, however, comes from the phonon-assisted quantum cutting (PQC) process and is primarily generated in low phonon energy crystal lattice field [16]. It is worthwhile to point out that luminescent signal includes emission from RE ions in glass host and fluoride nano-particles at luminescent spectra. In GCs, most of RE ions are incorporated in the fluoride crystal phase, which mainly emit red UC luminescence. Nevertheless, a part of RE ions exists in glass host and mainly emits green UC luminescence. As Fig. 3 shows, the ratio value of red and green UC luminescent intensities increase from 1:1.31 in GCs to 1:0.61 in nano-particles aqueous solution. The key reason for the red UC enhancement arises from the fact that the glass host is corroded by hydrofluoric acid, the fluoride nano-particles formerly embedded in glass matrix are released to aqueous solution and eventually red UC luminescent intensities increase sharply. These results are consistent with the conclusion drawn by XRD and TEM. The nano-particles in aqueous solution have the same luminescent properties as those existing in glass host.

From a practical point of view, it is possible for the nano-particles in aqueous solution from the GC-host to have a potential application as nano-sized probes used in the drug targeting after appropriate modification during the exploration of cellular and intracellular targeting. Under ideal circumstances, nano-particles for site-specific drug delivery, mediated by a targeting sequence, should deliver their payload only to specific target cells, tissues or organs [9, 18]. Moreover, nano-particles may optimize the bio-availability and the bio-distribution of the drug. The nano-particles in aqueous solution from the GC-host also apply in non-invasive imaging by detecting the luminescence of nano-particles inside biological systems, like cells, tissues or whole organisms. The further work for digging out the properties and applications of the nano-particles in aqueous solution is under way.

Conclusion

In summary, β-(Pb,Cd)F_2:Er^{3+},Yb^{3+} nano-particles in aqueous solution were prepared by means of thermal induction to produce nano-particles in glass matrix and corroding the glass host by hydrofluoric acid. The nano-particles in aqueous solution have the same structure and luminescent properties as nano-particles existing in glass matrix. Although thermal induction and corrosion treatment were used to prepare β-(Pb,Cd)F_2:Er^{3+},Yb^{3+} nano-particles in aqueous solution in this letter, it may directly apply to any other silicate GCs doped with other RE ions and embedded various composition of nano-particles, since the preparation method is based on a fundamental consideration.

References

1. Y. Wang, J. Ohwaki, Appl. Phys. Lett. **63**, 3268 (1993). doi:10.1063/1.110170
2. W. Luo, Y. Wang, Y. Cheng, Y. Cheng, F. Bao, L. Zhou, Mater. Sci. Eng. B **127**, 218 (2006). doi:10.1016/j.mseb.2005.10.034
3. F. Lahoz, I.R. Martín, U.R. Rodríguez-Mendoza, I. Iparraguirre, J. Azkargorta, A. Mendioroz, R. Balda, J. Fernández, V. Lavín, Opt. Mater. **27**, 1762 (2005). doi:10.1016/j.optmat.2004.11.047

4. M. Beggionra, I.M. Reaney, Appl. Phys. Lett. **83**(3), 467 (2003). doi:10.1063/1.1594842

5. J. Méndez-Ramos, V. Lavín, I.R. Martín, U.R. Rodríguez-Mendoza, V.D. Rodríguez, A.D. Lozano-Gorrín, P. Núñez, J. Appl. Phys. **94**(4), 2295 (2003). doi:10.1063/1.1592298

6. F. Liu, E. Ma, D.Q. Chen, Y.L. Yu, Y.S. Wang, J. Phys. Chem. B **110**, 20843 (2006). doi:10.1021/jp063145m

7. S. Sivakumar, F.C.J.M. van Veggel, M. Raudsepp, J. Am. Chem. Soc. **127**, 12464 (2005). doi:10.1021/ja052583o

8. B. Dong, D.P. Liu, X.J. Wang, T. Yang, S.M. Miao, C.R. Li, Appl. Phys. Lett. **90**, 181117 (2007). doi:10.1063/1.2735955

9. D.A. Groneberg, M. Giersig, T. Welte, U. Pison, Curr. Drug Targets **7**, 643 (2006). doi:10.2174/138945006777435245

10. L.Y. Wang, Y.D. Li, Comput. Chem. Eng. **24**, 2557 (2006)

11. L. Huang, T. Yamashita, R. Jose, Y. Arai, T. Suzuki, Y. Ohishi, Appl. Phys. Lett. **90**, 131116 (2007). doi:10.1063/1.2719028

12. D. Karmakar, S.K. Mandal, R.M. Kadam, P.L. Paulose, A.K. Rajarajan, T.K. Nath, A.K. Das, I. Dasgupta, G.P. Das, Phys. Rev. B **75**, 144404 (2007). doi:10.1103/PhysRevB.75.144404

13. T.R. Oliveira, L. de S. Menezes, Cid B. de Araújo, A.A. Lipovskii, Phys. Rev. B **76**, 134207 (2007). doi:10.1103/PhysRevB.76.134207

14. S. Bhattacharya, A. Ghosh, Phys. Rev. B **75**, 092103 (2007). doi:10.1103/PhysRevB.75.092103

15. H. Yu, L.J. Zhao, J. Meng, Q. Liang, X.Y. Yu, B.Q. Tang, J.J. Xu, Chin. Phys. **14**(9), 1799 (2005). doi:10.1088/1009-1963/14/9/019

16. H. Yu, L.J. Zhao, Q. Liang, J. Meng, X.Y. Yu, B.Q. Tang, L.Q. Tang, J.J. Xu, Chin. Phys. Lett. **22**(6), 1500 (2005). doi:10.1088/0256-307X/22/6/056

17. H. Yu, L.J. Zhao, J. Meng, Q. Liang, X.Y. Yu, B.Q. Tang, J.J. Xu, Chin. Opt. Lett. **3**(8), 469 (2005)

18. A.M. Derfus, W.C.W. Chan, S.N. Bhatia, Adv. Mater. **16**, 961 (2004). doi:10.1002/adma.200306111